

Proceedings of the Research Institute of Atmospheric,
Nagoya University, Vol. 36 (1989) – Research Report –

LARGE-SCALE PROPAGATION PROPERTIES
OF
AN INTERPLANETARY DISTURBANCE
IN ASSOCIATION WITH A “HALO” CORONAL MASS EJECTION
ON 27 NOVEMBER 1979

Takashi Watanabe, Takakiyo Kakinuma, Masayoshi Kojima
and
Rainer Schwenn*

Abstract

Propagation properties of an interplanetary disturbance in association with a halo coronal mass ejection (CME), which was observed with the Solwind coronagraph from 08:22 to 09:58 *UT* on 27 November 1979, are examined utilizing IPS and spacecraft observations. Detailed model-fitting showed that a dip of the propagation speed of the disturbance was situated in the radial direction of the heliospheric current sheet. Quick deceleration of the disturbance along the current sheet is suggested.

1. Introduction

Among a wide variety of morphological species of white-light coronal mass ejections (CMEs), “halo” CMEs, which are coronal structures of excess brightness of the solar corona nearly surrounding the occulting disk of a satellite-borne coronagraph, are particularly of interest because the interplanetary consequence of a CME of this type must collide with the earth in a “head-on” manner. One of the best examples of the CME of this type is a coronal event which was observed with the Solwind coronagraph during the interval from 08:22 to 09:58 *UT* on 27 November 1979, immediately after the disappearance of a quiescent solar filament near the solar disk center [Howard *et al.*, 1982]. A provisional study of the interplanetary manifestation of the CME was performed by Watanabe [1985] and Watanabe *et al.* [1986] using interplanetary scintillation (IPS) and spacecraft observations of the solar wind. The

* Max-Planck Institute für Aeronomie, Katlenburg-Lindau, D-3411, FRG

presence of quasi-spherical interplanetary disturbance with a dip of the propagation speed around the sun-earth line was suggested by these works on the basis of direct deductions from IPS observations. The principal purpose of the present report is to discuss three-dimensional propagation properties of the interplanetary disturbance in detail by applying a model-fitting [Watanabe *et al.*, 1986] to IPS and spacecraft observations.

2. Solar/Interplanetary Observations

First, we review briefly previous works concerning solar/interplanetary observations relevant to the halo CME on 27 November 1979.

a) CME

The halo CME in question was observed by the Solwind coronagraph on 27 November 1979 during the interval from 08:22 to 09:58 *UT*, in the range from about $4R_{\odot}$ to $8R_{\odot}$ [Howard *et al.*, 1982]. The expanding speed of the CME projected onto the plane of the sky is $600 \pm 50 \text{ km/s}$ for all position angles around the occulting disk. The frontal speed may be estimated if we assume that the expanding speed is constant and that the boundary of emission forms a cone of constant angular spread. Howard *et al.* [1982] obtained the frontal speed of 1160 km/s . They also suggested that deceleration of the outward motion of the CME took place at about $7R_{\odot}$.

b) Solar Activity

Since the halo CME had a symmetric appearance around the occulting disk of the Solwind coronagraph, it will be reasonable to assume that the solar counterpart of the CME would have been located near the solar disk center. The most remarkable solar phenomenon which took place immediately before the detection of the CME was sudden disappearance of a large north-south oriented quiescent filament with its center located at *N05W03*. According to H-alpha observations at Mitaka (Fig. 1), the filament disappeared at around 06:45 *UT* on 27 November 1979 [Watanabe, 1985]. A 1N solar flare apparently in association with the disappearance of the filament was observed at *N18E05* in a nearby active region, from 06:47 *UT*. One more 1N solar flare took place within the same active region, at *N14E05* from 07:22 *UT*. A soft X-ray LDE (long decay event) of a C1 class occurred on November 27 from about 06:30 *UT* to 12:00 *UT*. This event may be the soft X-ray signature of flares reported in the active region [Cane *et al.*, 1986]. Thus the solar source of the halo CME in question may be characterized by the disappearing solar filament and the associated small flares.

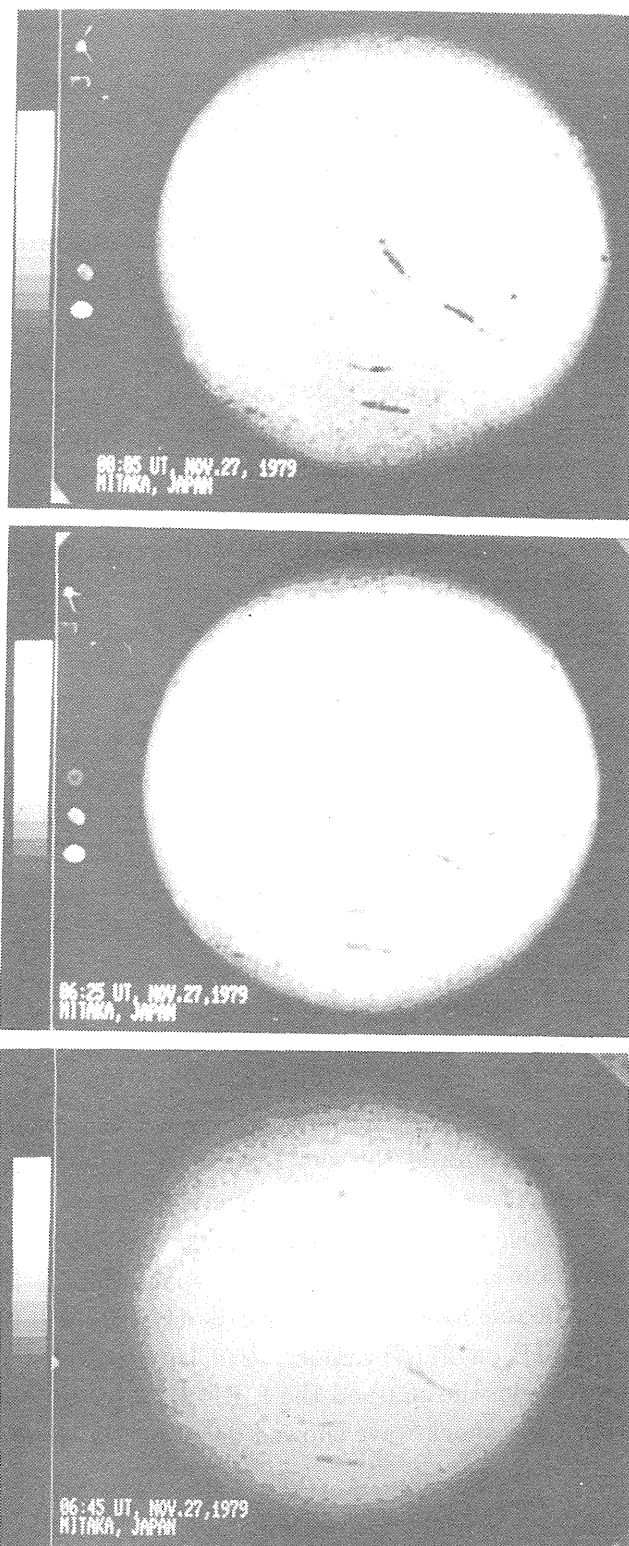


Fig. 1. Image-enhanced reproduction of H-alpha photographs taken at Mitaka, Tokyo at 00:05 *UT*, 06:25 *UT* and 06:45 *UT* on 27 November 1979. A large dark filament near the solar disk center disappeared between 06:25 *UT* and 06:45 *UT*, 27 November 1979.

c) *Interplanetary CME*

An interplanetary signature of the halo CME was observed with the zodiacal light photometers on board the Helios spacecraft as an outward-moving structure with an excess electron columnar density [Jackson, 1985]. At this time, Helios 2 was situated at 30° east of the sun-earth line $0.5AU$ from the sun. The Helios 2 photometers observed the interplanetary CME as it moved outward past the spacecraft at an altitude of 16° above the ecliptic plane. The approximate outward speed of the interplanetary CME was about $500km/s$, at around the heliocentric distance of $0.5AU$ [Jackson, 1985].

At the time of the mass ejection, Helios 1 was located at 120° east the sun-earth line $0.35AU$ from the sun. The southern portion of the interplanetary CME in question was also observed by the Helios 1 photometer on 27 November. Combining above-mentioned photometric observations, Jackson [1985] concluded that the CME moved outward directly along the sun-earth line and that it showed strong collimation in the north-south direction.

d) *Spacecraft Observations of Solar Wind*

An interplanetary shock wave was detected by Helios 2 (30° E, $0.5AU$), at about 16:00 UT on 28 November. The shock speed at the spacecraft is estimated to have been $550km/s$. It is reasonable to assume that the solar origin of the interplanetary shock wave was the disappearing filament or the halo CME on 27 November. The average shock speed between the sun and the spacecraft is about $630km/s$. It is concluded that the shock decelerated along the sun-Helios 2 line. The *in situ* shock speed at Helios 2 is consistent with the outward speed of the interplanetary CME near $0.5AU$ ($500km/s$) which was estimated by Jackson [1985]. Solar wind data obtained at Helios 1 (125° E, $0.35AU$) show no evidence of the shock wave at the spacecraft on 27-28 November.

The interplanetary shock wave in question was also observed at ISEE-1, -2, and -3 spacecraft. The arrival time of the shock wave at ISEE-3 was 06:49 UT on 30 November, immediately before an sc of geomagnetic storm at 07:38-07:41 UT on 30 November. The shock speed near the earth, which has been determined by using solar wind observations obtained with these three spacecraft, is $404km/s$ [Russell *et al.*, 1983]. The most probable solar origin of the shock wave will be the disappearing filament or the halo CME on 27 November 1979 [Howard *et al.*, 1982]. Since the average shock speed between the sun and the ISEE-3 spacecraft was about $560km/s$, it is also concluded that the shock wave showed deceleration along the sun-earth line.

e) *IPS Observations of Solar Wind*

The interplanetary disturbance in association with the halo CME was also detected by interplanetary scintillation (IPS) observations of radio sources as a tran-

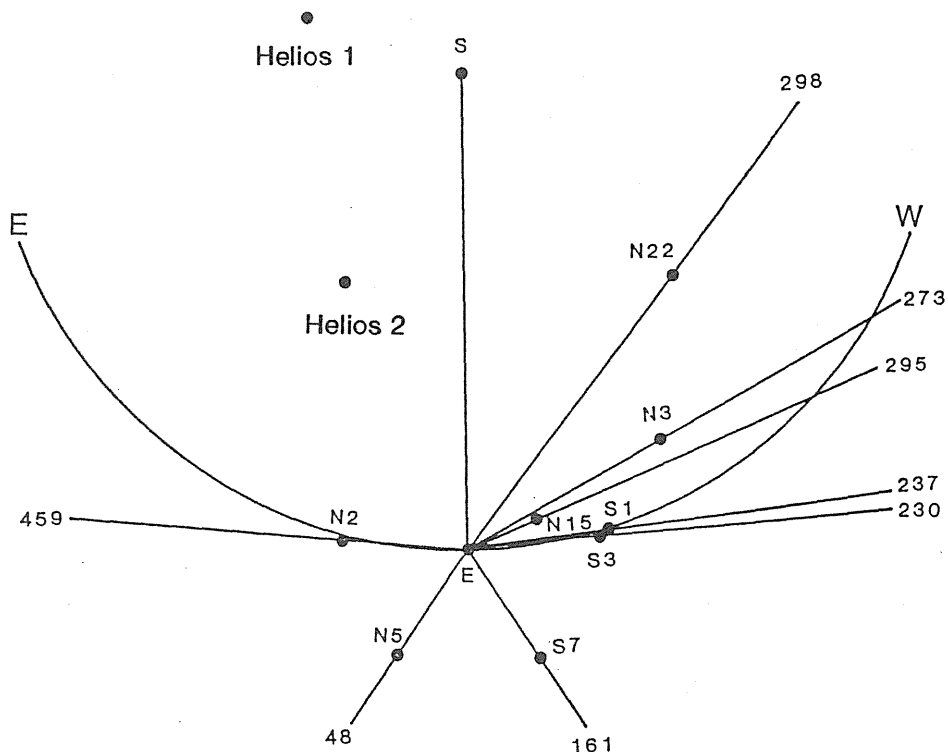


Fig. 2. Line-of-sight geometry on 30 November 1979 (projected onto the ecliptic plane). Locations of spacecraft are also shown.

sient increase in the flow speed accompanied with the enhancement of the scintillation level. The line-of-sight geometry on 30 November 1979 is shown in Fig. 2. IPS observations obtained at UCSD [Coles and Rickett, 1979] and Toyokawa are available. According to the direct deduction from IPS and spacecraft observations, the general three-dimensional configuration of the interplanetary disturbance in association with the halo CME may be approximated by a sphere having a dip of the shock speed around the sun-earth line [Watanabe, 1985; Watanabe et al., 1986b].

3. Empirical Modeling

Although IPS techniques enable us to obtain solar wind data in the region away from the ecliptic plane, it is somewhat difficult to study transient interplanetary disturbances utilizing IPS observations because the time resolution of current IPS observations is generally poor, and observational parameters, e.g., the solar wind speed, are affected by the line-of-sight integration. In previous works [Watanabe, 1985; Watanabe et al., 1986], it was assumed that the observed flow speed by IPS observation

is that of the plasma speed of the disturbance. This simple method is useful to see large-scale propagation properties of interplanetary disturbances, but it is necessary to take into consideration the above-mentioned limitation in IPS observations. A model fitting procedure [Watanabe *et al.*, 1986a] has been introduced to improve the situation. In this section, we find the best-fit model by which IPS and spacecraft observations in late November 1979 can be explained.

a) Method

We define the directivity of an interplanetary shock wave, $D(L,B)$, as a function of the longitude L (deg.) and the latitude B (deg.):

$$D(L, B) = F(L, B) \cos M(L - L_0) \cos N(B - B_0) \quad (1)$$

where

$F(L, B)$: reduction factor
 L_0 : longitude of the shock wave center (deg.)
 B_0 : latitude of the shock wave center (deg.)
 M, N : multiplication factors

We set $D(L, B) = 0$ when it has negative values. The reduction factor is newly introduced to represent the detailed geometry of the interplanetary disturbance. By using the directivity, the angular distribution of the total shock speed (shock speed plus ambient flow speed) of an interplanetary disturbance is given by the formula:

$$VS(L, B, R) = VS_0 D(L, B) (R/R_0)^{-DE} + V_0(L, B) \quad (2)$$

where

$VS(L, B, R)$: total shock speed (km/s)
 R : heliocentric distance (AU)
 VS_0 : initial shock speed (km/s) at ($L_0 = 0, B_0 = 0$)
 R_0 : heliocentric distance of the initial point (AU)
 DE : power-law deceleration coefficient
 $V_0(L, B)$: ambient solar wind speed (km/s)

The radial thickness of the interplanetary disturbance, $DS(L,B)$ in AU , is defined as follows:

$$DS(L, B) = DS_0 D(L, B) \quad (3)$$

where DS_0 is the maximum radial thickness in AU . Since we simulate IPS observation near $1 AU$, we neglect the radial evolution of the thickness. By using the above-mentioned empirical model of the interplanetary disturbance, we predict the flow speed to be observed by IPS observation taking into account the line-of-sight integration. To do this we assume the extended medium weak scattering [Coles and Harmon, 1978]. Since the observed speed is essentially the line-of-sight average of the plasma speed, we assume that the plasma speed in the post-shock region is 80% of the shock speed given by eq. (2), after the strong-shock approximation for an ideal gas. We also assume that the level of electron density fluctuations within the disturbance is 5 times as high as the ambient level and that the levels of electron density fluctuations are proportional to R^{-2} .

*b) Empirical Model of Interplanetary Disturbance
in Association with Halo CME on 27 November 1979*

As the first step of the modeling, we assume the angular distribution of the ambient solar wind, $V_0(L,B)$. Since the number of observation points in interplanetary space is not sufficient to determine the geometry of stream structures of the ambient solar wind at a given instance, we adopt an observational deduction that the low-speed solar wind tends to appear along the heliospheric current sheet and that the high speed streams appear above the photospheric regions with predominantly the same magnetic polarity; i.e. coronal holes [e.g., Kojima and Kakinuma, 1987]. For this purpose, we employed synoptic charts of the heliospheric magnetic field published by Hoeksema and Scherrer [1983]. Solar wind speeds are selected to be consistent with the flow speeds observed immediately before the arrival of the interplanetary disturbance at observational points. The assumed angular distribution of the ambient solar wind speed at $1 AU$ on 30 November is given in Fig. 3.

By using the angular distribution of the ambient solar wind speed given in Fig. 3, we determine the first-order model of the interplanetary disturbance near the ecliptic plane on the basis of Helios 2 and ISEE-3 observations. We assume that the interplanetary disturbance departed the sun at 07:00 UT on 27 November, which is inferred from H-alpha observations at Mitaka [Watanabe, 1985]. Since it is not the purpose of the present study to model the interplanetary disturbance near the sun, we neglect acceleration of the ambient solar wind. For the initial speed of the shock wave, we assume that $VS_0 = 830 km/s$. This gives the total shock speed (shock speed plus ambient flow speed) of $1160 km/s$, which is equal to the frontal speed of the CME estimated by Howard *et al.* [1982], for the ambient flow speed of $330 km/s$.

We then simulate the shock wave characteristics observed at Helios 2 ($R = 0.5AU$, $L = -30^\circ$). Observations are simulated fairly well as shown in Fig. 4 by assuming the following parameters; $F(L,B) = 1$, $M = 1.5$, $N = 1.5$, $L_0 = +05^\circ$, $B_0 = +05^\circ$, $DE = 0.5$, and $DS = 0.15$. This means that the shock wave showed a blast-shock like deceleration between the solar corona and Helios 2. The shock wave

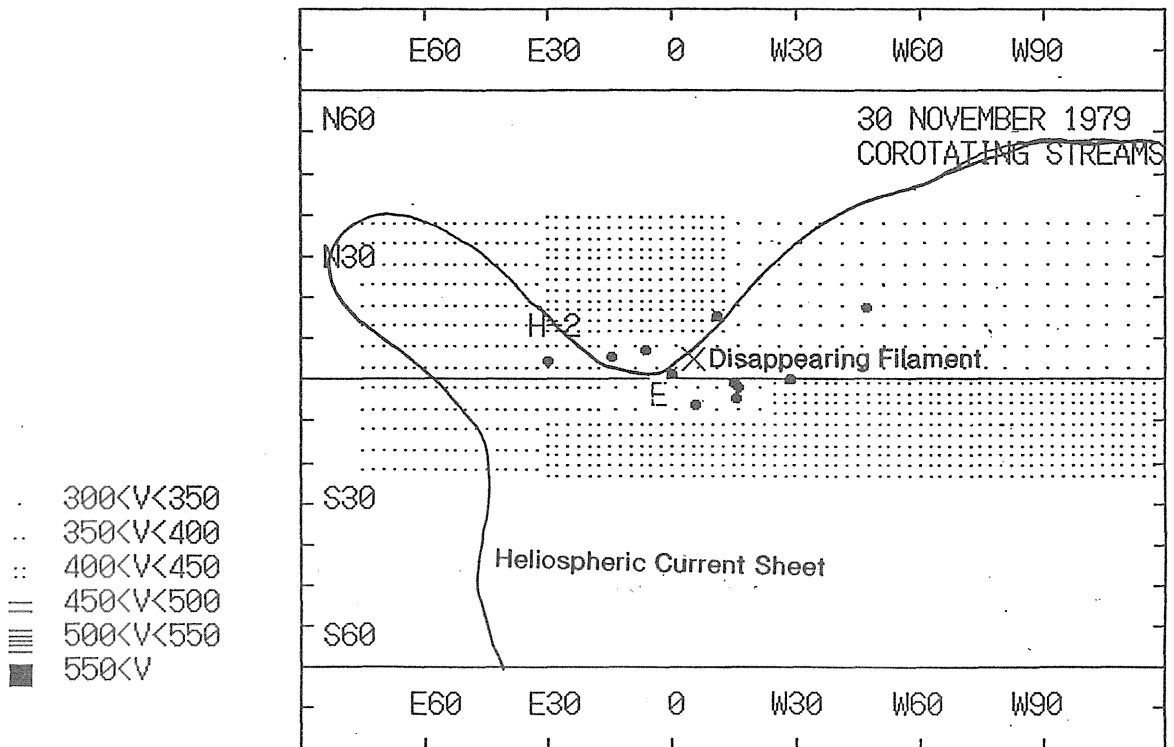


Fig. 3. Assumed angular distribution of the ambient solar wind speed on 27-30 November 1979. The longitude is measured from the central meridian of the sun, and the latitude is measured from the solar equatorial plane. Location of the center of the scattering weighting function on each line of sight is indicated by a dot. The locations of spacecraft are also indicated.

observations at ISEE-3, near 1 AU, cannot be predicted by the same model employed to predict Helios 2 observations, because this model gives too fast shock speed at ISEE-3. It is necessary to assume both a slower initial shock speed and a larger deceleration coefficient than those assumed in prediction of Helios 2 observations. We adopt the reduction factor of $F(L, B) = 0.9$ along the sun-earth line, and employ a larger value of the deceleration coefficient of $DE = 0.7$. The result of prediction is shown in Fig. 5. It is suggested that the angular distribution of the shock speed had a dip along the sun-earth line.

The first-order model, which has been determined by using spacecraft observations, is now applied to IPS observations to construct a three-dimensional model. We try to obtain the best-fit model in an iterative manner. Solar wind data obtained with IPS observation of 3C298 are particularly important to know dynamic properties of the shock wave in the region to the west of the sun-earth line, above the solar equatorial plane. As shown in Fig. 6, IPS speeds obtained with IPS observations of 3C298 are well predicted by assuming $F(L, B) = 1$, $DE = 0.5$, and $M = 1.0$.

IPS observations of 3C273 and 3C237 are important to determine the angular spread of the dip in the shock speed in the region to the west of the sun-earth line, near the solar-equatorial plane. As shown in Fig. 7, IPS observations of 3C273 are well predicted if we assume that the dip is distributed over the longitudes of $0^\circ - +40^\circ$ and the latitude of $\pm 10^\circ$. The power-law deceleration coefficient within the dip is taken to be 0.7, the same value that has been introduced to simulate near-earth spacecraft observations. This model is also consistent with IPS observations of 3C237 near 1AU (Fig. 8). We tentatively assume that the dip has an extent of 10° in the eastern hemisphere. The prediction for IPS observations of 3C459 is shown in Fig. 9.

Propagation properties of the shock wave in the region to the north of the earth can be examined by using IPS observations of 3C295. As shown in Fig. 10, the highly disturbed solar wind with the speed of about 500km/s was observed on early 30 November. Since the observed plasma speed is considerably faster than the post-shock flow speed near the earth (about 370km/s), it is suggested that the dip of the shock speed around the sun-earth line was confined in the region around the ecliptic plane. The extent of the hole in the northern hemisphere is necessary to be smaller than 15° to simulate IPS observations of 3C295.

Concerning the southern hemisphere, it is somewhat difficult to obtain a comprehensive model because of the small number of IPS sources to observe the region to the south of the ecliptic plane. In the interval of our interest, IPS observations of only one radio source, 3C161, are available. The disturbed solar wind was observed by IPS observation of this radio source at UCSD and at TYKW on 30 November 1979, shortly after the arrival of the shock wave at ISEE-3 (06:49 UT). If we take into consideration the fact that the peak of the principal scattering zone along the line-of-sight of this radio source was located at about 0.3AU outside the earth's orbit, it is suggested that the shock wave propagated with greater speed than that

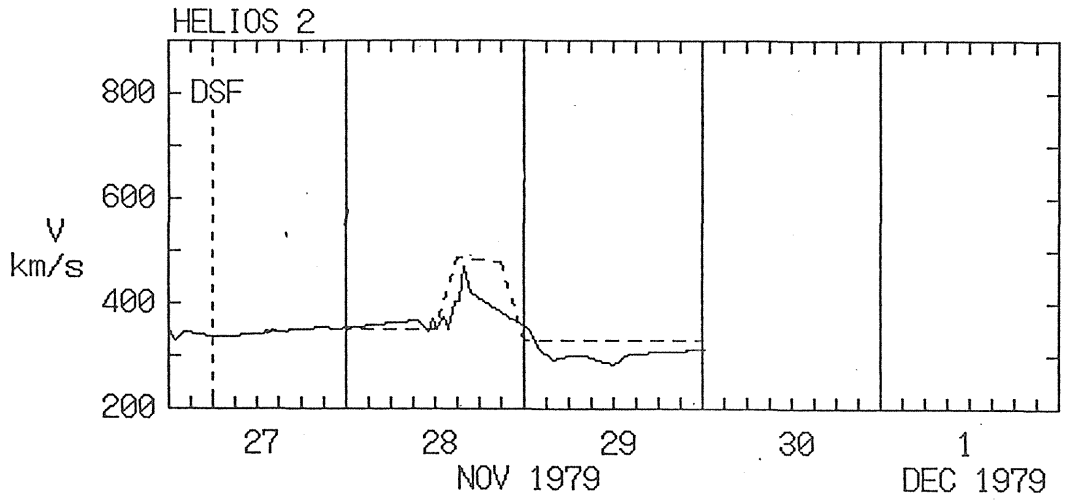


Fig. 4. Comparison between the observed time variation of the flow speed at Helios 2 (solid line) and prediction (broken line).

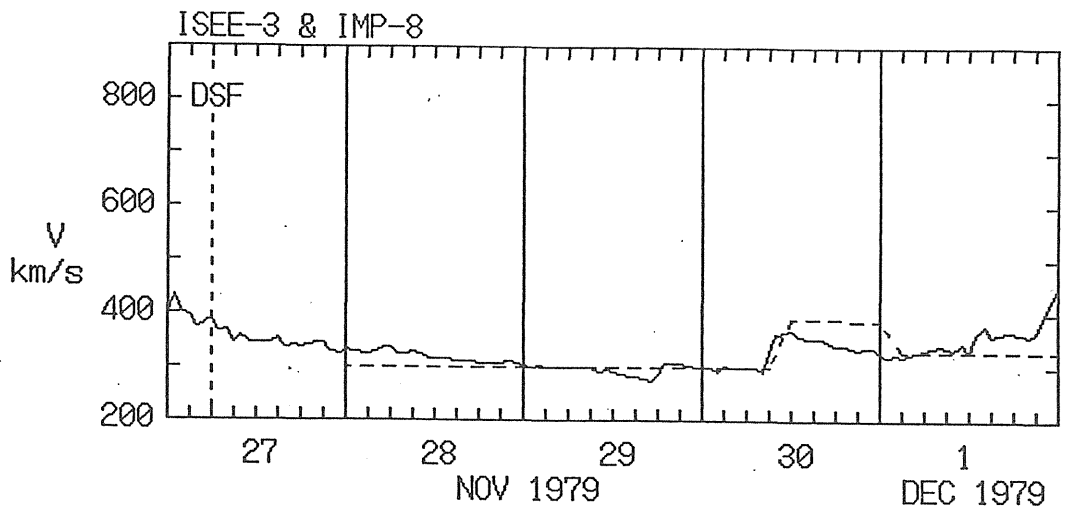


Fig. 5. Same as Fig. 4 but for ISEE-3.

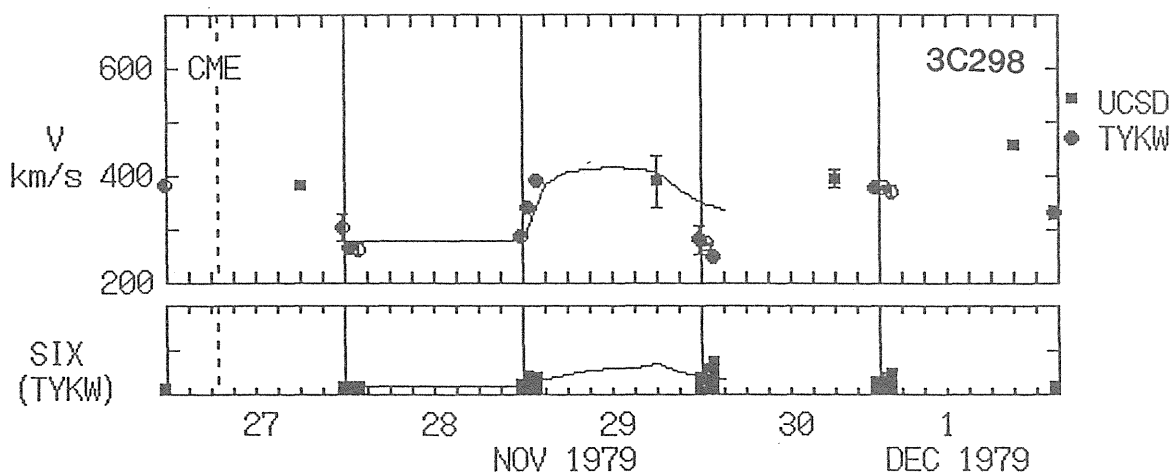


Fig. 6. Comparison between flow speeds obtained by IPS observations of 3C298 (dots) and the predicted time variation of the flow speed (broken line). The lower panel (SIX) shows the level of scintillation observed at Toyokawa (TYKW), in arbitrary units.

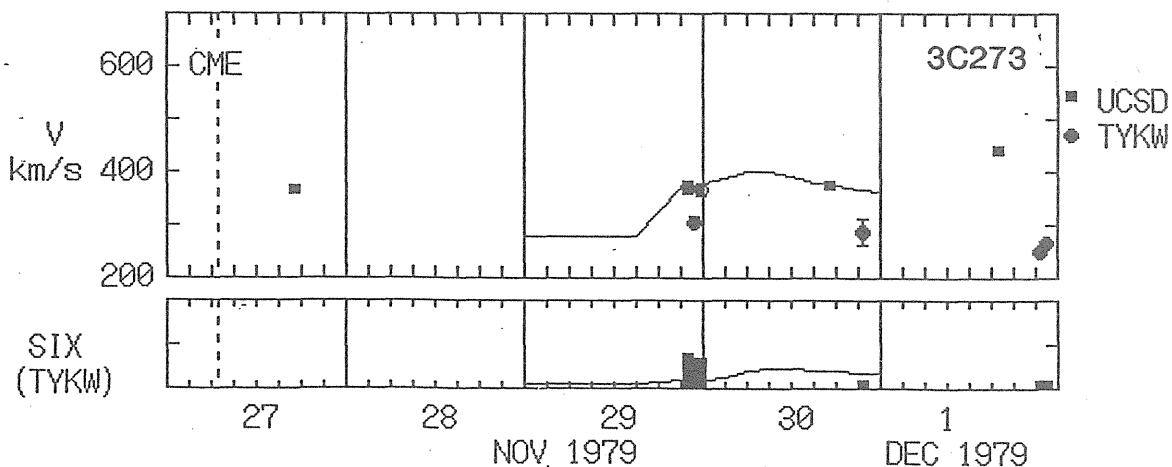


Fig. 7. Same as Fig. 6 but for 3C273.

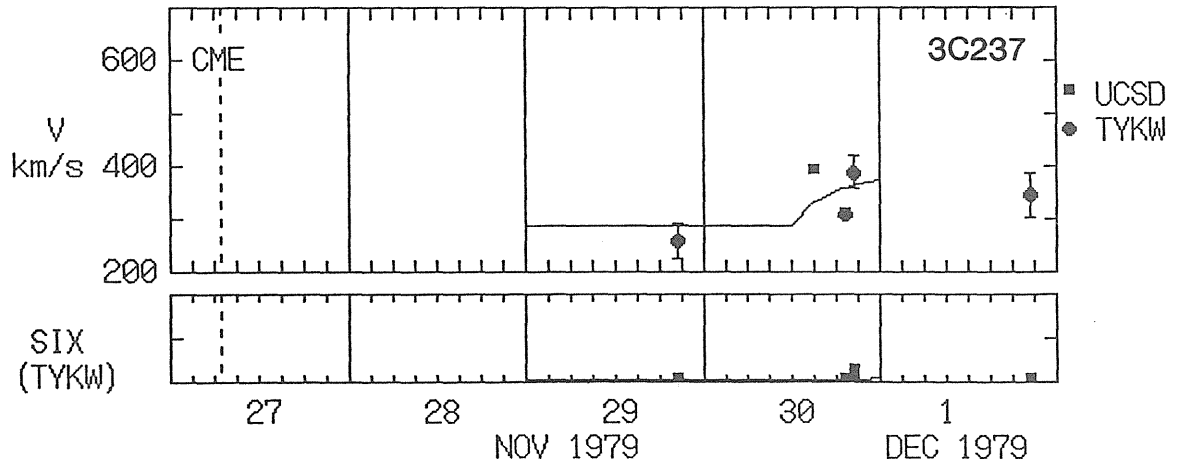


Fig. 8. Same as Fig. 6 but for 3C237.

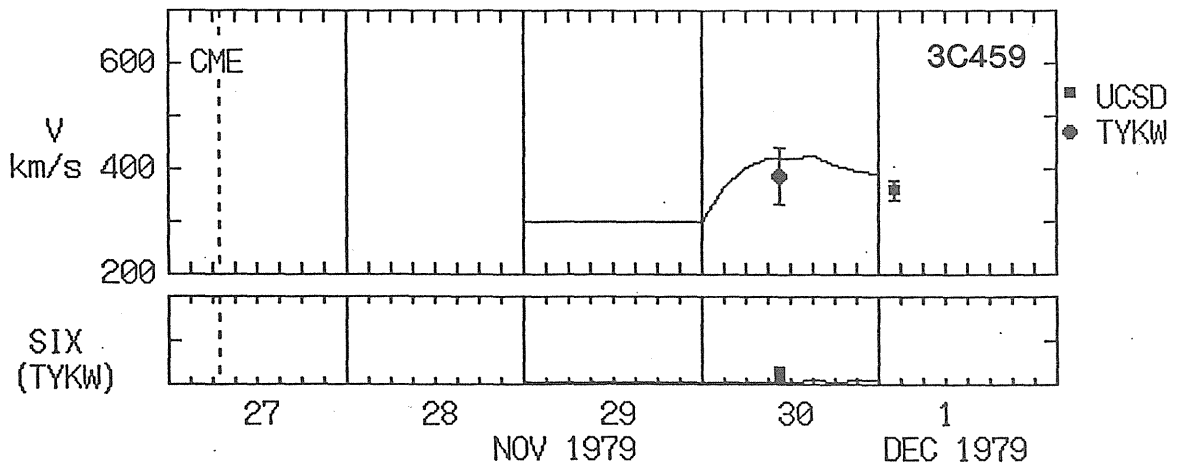


Fig. 9. Same as Fig. 6 but for 3C459.

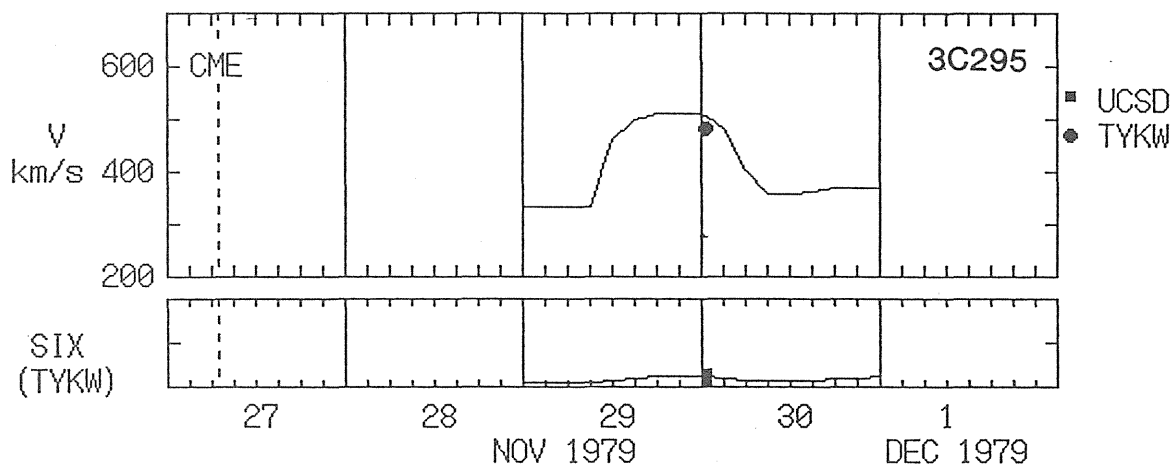


Fig. 10. Same as Fig. 6 but for 3C295.

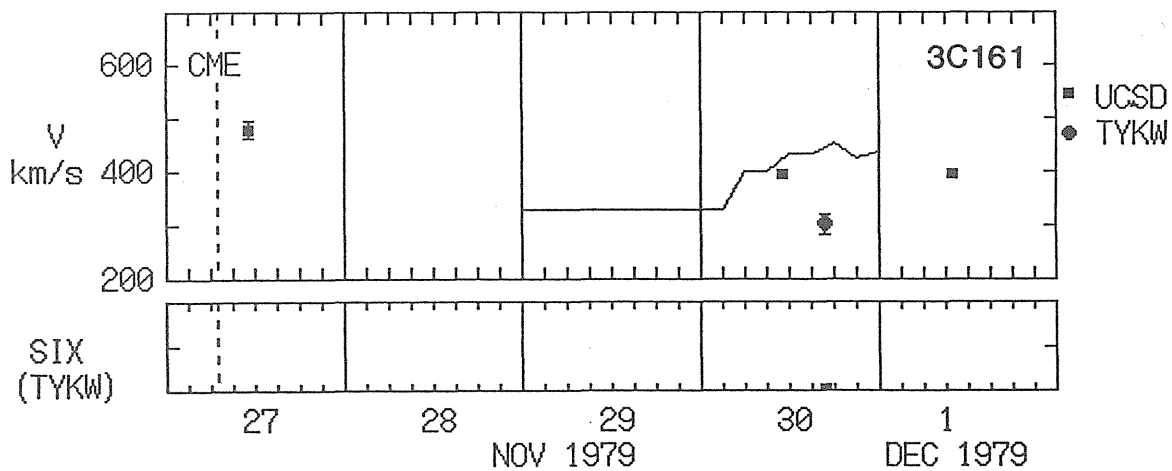


Fig. 11. Same as Fig. 6 but for 3C161.

along the sun-earth line. To simulate IPS observations of 3C161 on 30 November – 1 December, it is necessary to assume a smaller deceleration coefficient ($DE = 0.3$), because Solwind CME observations suggest that the initial shock speed in the southern hemisphere would have been similar to that in the northern hemisphere. Parameters employed in the above-mentioned modeling are summarized in Table 1.

Table 1. Parameters which determine dynamic characteristics of the interplanetary disturbance in association with halo CME on 27 November 1979

Region	M	N
L>5	1	1.5
L<5	1.5	1.5

Region	V_0	N	F(L,B)
L<-20, B>+10	350	0.5	1
L<-10, -10<B<+10	350	0.5	1
L<-30, B<-10	350	0.5	1
-30<L+15, B>+10	400	0.5	1
L<+20, B>+10	300	0.5	1
-10<L<+40, -10<B<+10	300	0.7	0.9
L>+40, 0<B<+10	300	0.5	1
L>+40, B<0	400	0.5	1
-30<L<+40, B<-10	400	0.3	1

c) Three-Dimensional Geometry of Shock Wave

in Association with Halo CME on 27 November 1979

An approximate three-dimensional geometry of the shock wave in question is constructed on the basis of the model-fitting performed in the previous section. Location of the leading edge (the shock front) of the interplanetary disturbance in the interval from 28 November to 1 December 1979 at 00:00 UT for each date is schematically shown in Fig. 12a (the ecliptic-plane cross section) and in Fig. 12b (the central-meridian plane cross section). The dip which is formed around the sun-earth line is evident. The large-scale configuration of the interplanetary disturbance derived from present model-fitting is largely consistent with that given by previous direct deductions [Watanabe, 1986; Watanabe *et al.*, 1986].

The two-dimensional distribution of the shock speed at 1AU is also illustrated in Fig. 13. It is seen that the high-speed portion appeared in the region apart from

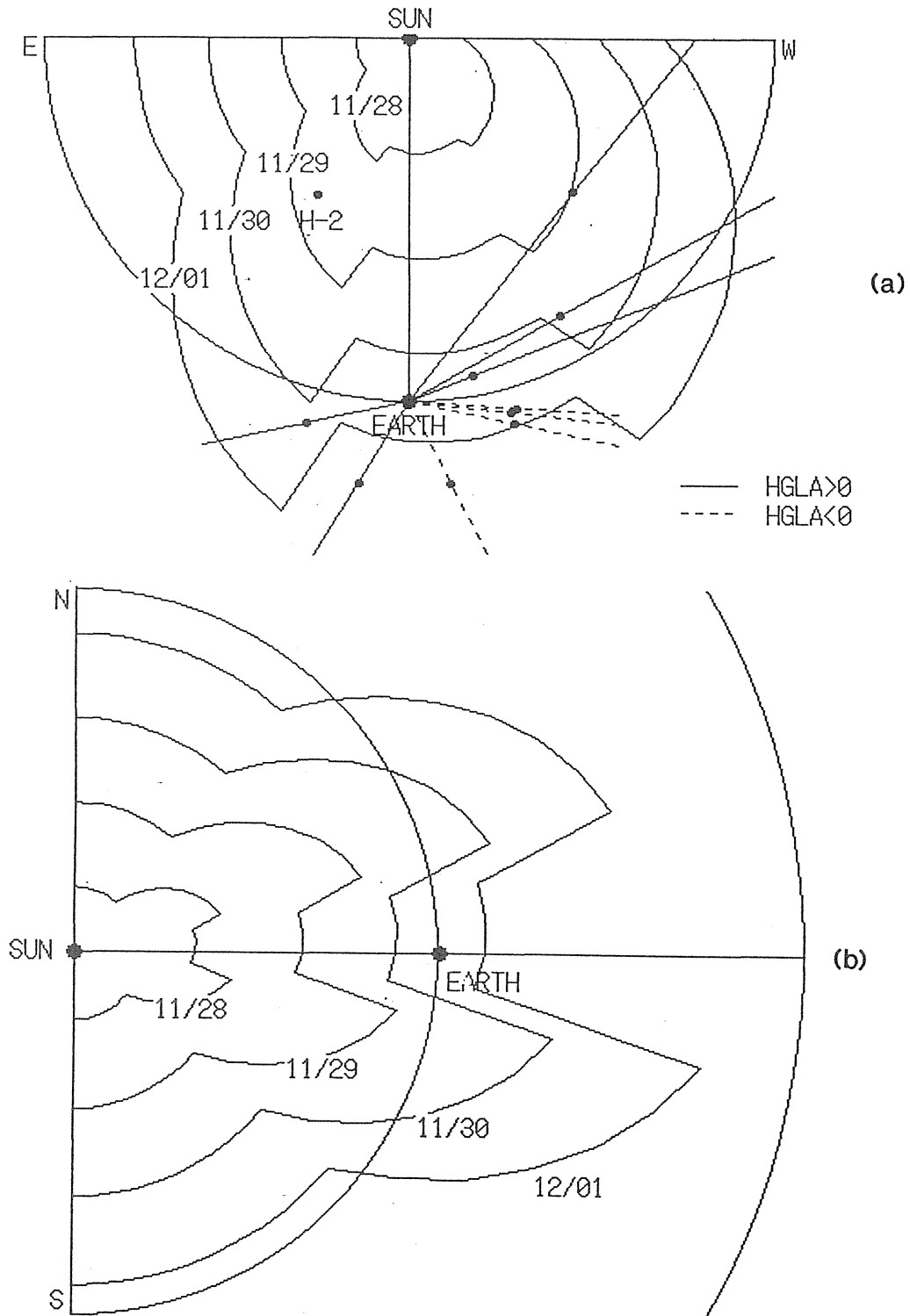


Fig. 12. Approximate configuration of the leading edge of the interplanetary disturbance in association with the disappearing filament on 27 November 1979, at 00:00 UT on each date. Upper panel (a) shows the equatorial cross section; lower panel (b) shows the central meridian cross section.

the solar-equatorial plane, both in the northern and the southern hemisphere. The dip of the shock speed appeared in the radial direction of the heliospheric current sheet, near the normal of the disappearing solar filament.

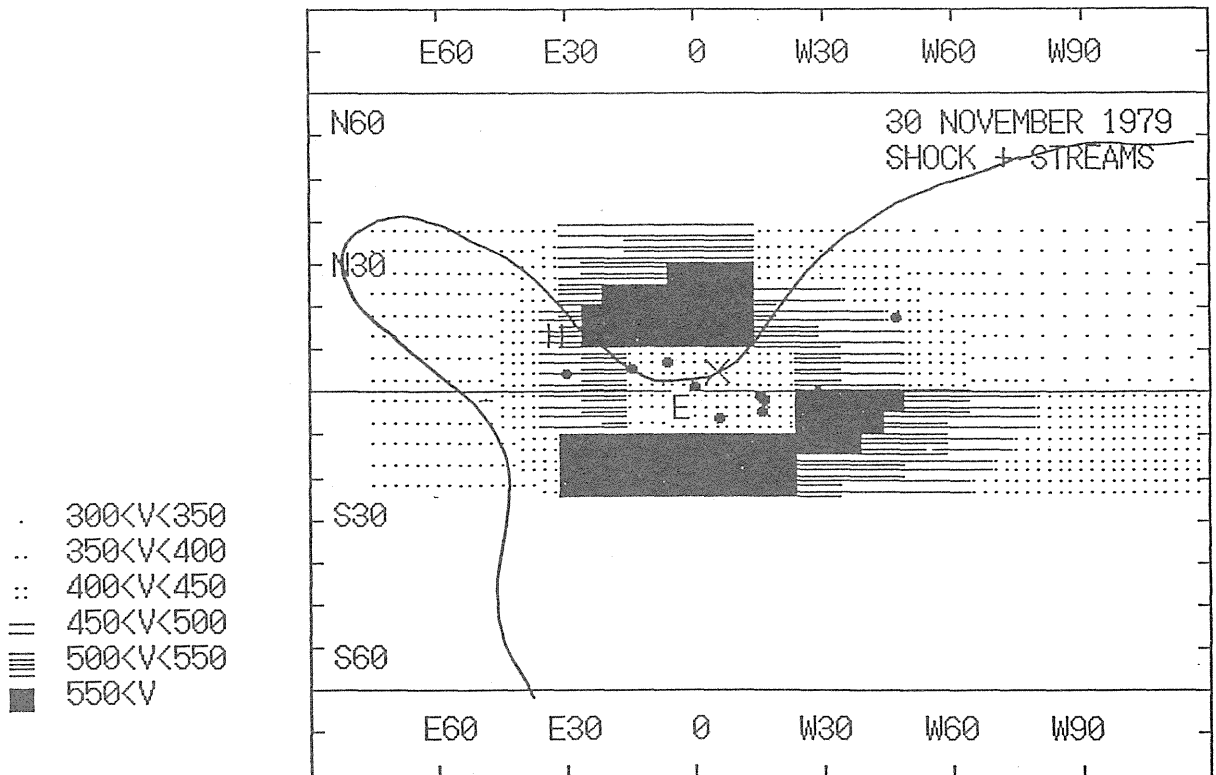


Fig. 13. Angular distribution of the plasma speed at $1AU$ on 30 November 1979. An enhancement of the plasma speed which is seen around the radial direction of the earth is caused by the interplanetary disturbance in association with the disappearing filament on 27 November 1979.

4. Concluding Remarks

It is apparent that the empirical model of the interplanetary disturbance in association with the halo CME on 27 November 1979 is not unique, because many other combination of the parameters are conceivable. Nevertheless, it is possible to give constraints to the model as follows.

1. A quasi-spherical interplanetary disturbance was generated in association with the halo CME observed with the Solwind coronagraph from 08:22 *UT* on 27 November, or a disappearing filament which was observed near the solar

disk center immediately before the detection of the CME.

2. The center of the disturbance was located around the sun-earth line, near the radial direction of the disappearing filament.
3. A local depression of the propagation speed of the interplanetary disturbance was situated around the sun-earth line. The deceleration of the disturbance was strong around the line.

Since the low-latitude portion of the heliospheric current sheet was located near the sun-earth line, it is suggested that the presence of the current sheet is responsible to form the dip of the interplanetary disturbance around the sun-earth line. The slower ambient solar wind and the stronger deceleration along the current sheet will result in the dip. A similar result was obtained for an interplanetary disturbance in association with the disappearing solar filament on 23 May 1979 [Watanabe *et al.*, 1988]. In conclusion, the presence of the heliospheric current sheet will play an important role to determine detailed dynamical characteristics of interplanetary disturbances. Henning *et al.* [1985] also suggested that interplanetary disturbances are weakened by interaction with the heliospheric current sheet.

Acknowledgment

The authors acknowledge valuable comments on the manuscript received from K. Marubashi of the Communications Research Laboratory, Ministry of Post and Telecommunications.

References

- Cane, H. V., S. W. Kahler, and N. R. Sheeley, Jr., Interplanetary Shocks Preceded by Solar Filament Eruptions, *J. Geophys. Res.*, **91**, No. A12, 13321-13329, 1986.
- Coles, W. A., and B. Rickett, Solar-Geophysical Data, No. 424, Part 1, December, 1979, U. S. Department of Commerce, Boulder, Colorado, U. S. A.
- Coles, W. A., and J. K. Harmon, A. J. Lazarus, and J. D. Sullivan, Comparison of 74-MHz interplanetary scintillation and IMP 7 observations of the solar wind during 1973, *J. Geophys. Res.*, **83**, 3337-3341, 1978.

- Henning, H. M., P. H. Scherrer, and J. T. Hoeksema, *J. Geophys. Res.*, **90**, 11055-11061, 1985.
- Howard, R. A., D. J. Michels, N. R. Sheeley, Jr., and M. J. Koomen, The observation of a coronal transient directed at earth, *Astrophys. J.*, **263**, L101-L104, 1982.
- Jackson, B. V., Helios observations of the earthward directed mass ejection of 27 November, 1979, *Solar. Phys.*, **95**, 363-370, 1985.
- Kojima, M., and T. Kakinuma, Solar Cycle Evolution of Solar Wind Speed Structure Between 1973 and 1985 Observed With the Interplanetary Scintillation Method, *J. Geophys. Res.*, **92**, 7269-7279, 1987.
- Russell, C. T., E. J. Smith, B. T. Tsurutani, J. T. Gosling, and S. J. Bame, Multiple spacecraft observations of interplanetary shocks: characteristics of the upstream ULF turbulence, in *Solar Wind Five*, ed. M. Neugebauer, NASA CP-2280, pp.365-400, 1983.
- Watanabe, T., Interplanetary manifestation of the "halo" coronal mass ejection of November 27, 1979, *Proc. Res. Inst. Atmospheric, Nagoya Univ.*, **32**, 11-28, 1985.
- Watanabe, T., and R. Schwenn, Large-scale propagation properties of interplanetary disturbances revealed from IPS and spacecraft observations, *Space Sci. Rev.*, in press, 1989.
- Watanabe, T., T. Kakinuma, and M. Kojima, Empirical modeling of interplanetary disturbances, *Adv. Space Res.*, **6**, No. 6, 331-334, 1986a.
- Watanabe, T., T. Kakinuma, and M. Kojima, Three-dimensional configurations of interplanetary disturbances associated with coronal mass ejections, in *The Sun and the Heliosphere in Three Dimensions*, ed. R. G. Marsden, Reidel, pp.123-128, 1986b.
- Watanabe, T., T. Kakinuma, and M. Kojima, Radio Scintillation Observations of Interplanetary Disturbances in Association with Solar Filament Activity, in *Laboratory and Space Plasmas*, ed. K. Kikuchi, Springer-Verlag, Berlin, pp.399-414, 1988.